Characteristics of transmission of electrons in a bent quantum waveguide with inhomogeneous magnetic fields

Ben-Yuan Gu, Yuh-Kae Lin, and Der-San Chuu

Citation: Journal of Applied Physics **86**, 1013 (1999); doi: 10.1063/1.370840
View online: http://dx.doi.org/10.1063/1.370840
View Table of Contents: http://scitation.aip.org/content/aip/journal/jap/86/2?ver=pdfcov
Published by the AIP Publishing

Characteristics of transmission of electrons in a bent quantum waveguide with inhomogeneous magnetic fields

Ben-Yuan Gu
Institute of Physics, Chinese Academy of Sciences, P.O. Box 603, Beijing 100080, People's Republic of China

Yuh-Kae Lin and Der-San Chuu[a)]
Department of Electrophysics, National Chiao Tung University, Hsinchu, 30050, Taiwan

(Received 24 November 1998; accepted for publication 6 April 1999)

We present numerical studies of the transmission properties in an L-shaped quantum waveguide (LQW) subject to an inhomogeneous magnetic field perpendicular to the LQW plane. The magnetic field remains zero at the corner region, thus, a magnetically defined cavity is formed in this LQW. We find that transmission characteristics of electrons in the LQW depend strongly on geometric parameters and magnetic configurations. Sharp peaks with unity amplitude and deep dips are observed in transmission as a function of the Fermi energy of the incident electron at some high fields. The mode–mode coupling between the wires and the cavity and multiple reflection of electrons in the cavity lead to the appearance of these structures in transmission spectrum. We also study the variation of transmission with magnetic field for different magnetic confinement configurations when fixing incident electron energy. In the magnetic depletion process of the propagating modes in wires, the transmission exhibits various patterns, such as stepped drop, wide valley, deep dips, large oscillations, or without any structure, sensitively dependent on incident electron energy and magnetic confinement configurations. It is expected that one can flexibly modify transmission spectrum of the LQW by applying an inhomogeneous magnetic field to match practical requirements. © *1999 American Institute of Physics.* [S0021-8979(99)05714-X]

I. INTRODUCTION

In past decades, advancements of nanolithography have made possible the fabrication, in practice, of various confinement structures in a two-dimensional electron gas (2DEGS) through built-in control grid patterns, such as quantum wires, dots, or rings on a mesoscopic size. In these structures, the characteristic scale of the system at least in some dimension is comparable to the Fermi wavelength of electron. Thus, the transport behavior of electron is characterized by the ballistic one.[1] The quantum interference effect becomes more pronounced. It leads to the manufacture of new concept devices with operation principle entirely based on quantum interference phenomena, such as a transistor based on resonant tunneling effect,[2,3] the T-shaped electronic waveguide,[4] the coupled dual-quantum waveguides,[5–12] bent waveguides,[13–17] etc.

Electron transport properties under the application of magnetic fields have also attracted much attention and wide investigations in recent years.[18–31] In these cases, the current-carrying edge states play an important role in determining the electron transport behaviors in devices. These edge states are formed near the boundary regions or the interfaces in which the abrupt change of the magnetic fields in magnitude or polarity appears. A variety of new phenomena are expected in these structures.

Since the interconnection of quantum devices is usually achieved through a bend, it is necessary to study the problem of bending resistance. It is well known that the sharp corner and junctions may cause severe reflection of the incoming electrons, especially in two spatial dimensions.[4,14–16] It is desirable to design bent quantum wires with little reflections. A few research groups have devoted to these studies.[4,13–19] They found that the reflection of electrons could be reduced to zero if the bending radius in the circularly bent two-dimensional quantum wires are large enough.[4,13] The other scheme was proposed by Wang *et al.*[17] They suggested an interconnection block which is a two-dimensional L-shaped quantum wire where a double potential barrier is placed at the corner. The localized state[4,14–16] at the corner region without the barriers is pushed into the continuum in the presence of the barriers, resulting in resonant tunneling. Therefore, the reflection at the corner can be eliminated through resonant tunneling.

Motivated by these works, in this article we propose another possible design: creating a magnetically defined quantum cavity at the corner region through applying an inhomogeneous magnetic field perpendicular to an L-shaped quantum waveguide (LQW) plane. Thus, the mode–mode coupling between the cavity and wires can be substantially changed. It leads to various transmission spectra of the LQW, including sharp peak-dips structures. We will reveal the effects of various geometric and magnetic configurations on the transmission properties of the LQW in detail.

This article is organized as follows: Section II gives a brief description of the model device structure and the necessary formulas used in calculations. The calculated results

[a)]Electronic mail: dschuu@cc.nctu.edu.tw

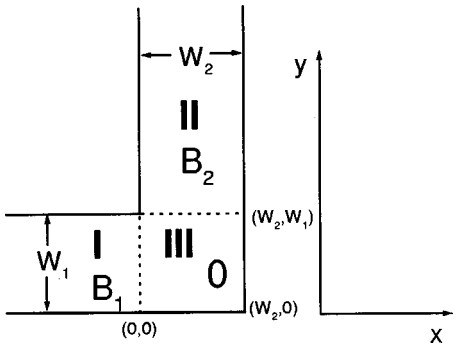

FIG. 1. Sketch of an L-shaped two-dimensional electron waveguide subject to an inhomogeneous magnetic field.

and discussions are presented in Sec. III. Finally, a brief summary is given in Sec. IV.

II. MODEL AND FORMULAS

We consider an L-shaped two-dimensional electron waveguide, lying on the X-Y plane, i.e., the bend angle is 90°. The transmission properties of electrons in an LQW, which was subjected to an inhomogeneous magnetic field perpendicular to the quantum waveguide plane and a magnetically confined cavity is formed at the corner region, will be studied for various geometrical parameters and magnetic configurations. Experimentally, inhomogeneous magnetic fields on the nanometer scale can be established with, for instance, the creation of magnetic dots,[31] the patterning of ferromagnetic materials,[32,33] and the deposition of superconducting materials on heterostructures.[34] The LQW can be divided into three subregions: a horizontal wire with a width of W_1 (region I), a bent region with an area of $W_1 \times W_2$ (region III), and a vertical wire with a width of W_2 (region II), as shown in Fig. 1. For simplicity, the magnetic field is assumed to be uniform in each individual subregion and can be denoted as B_1 in region I, B_2 in region II. On the corner region, the magnetic field is always zero, leading to the formation of a magnetically confined cavity. We employ, for simplicity of calculations, the hard-wall confinement potential for boundaries. The transverse potential inside the LQW is set to zero. We choose the Landau gauge for the vector potential in different regions as

$$\mathbf{A}(x,y)=\begin{cases}(0,B_1x)=(-B_1y,0)+\nabla B_1xy, & \text{in region I;}\\ (-B_2(y-W_1),0)=(0,B_2x)-\nabla B_2x(y-W_1), & \text{in region II;}\\ (0,0), & \text{in region III.}\end{cases} \tag{1}$$

It can be noted that this form of the gauge guarantees the continuity of the vector potential at every interface.

In the effective mass approximation, a boundary matching method[14] can be employed to solve the Schrödinger equation of the single electron in the presence of an inhomogeneous magnetic field. We write down the wave functions in individual regions, and match the boundary conditions by requiring that the wave functions and their normal derivatives must remain continuous at each interface. The electron wave functions can be expressed as the following when an electron is incident through mode n in region I. They are

$$\Psi_n^{\mathrm{I}}=e^{-ixy/l_{B_1}^2}[e^{ik_n^{\mathrm{I}(+)}x}\Phi_n^{\mathrm{I}(+)}(y)+r_{mn}e^{ik_m^{\mathrm{I}(-)}x}\Phi_m^{\mathrm{I}(-)}(y)] \tag{2a}$$

in region I, and

$$\Psi_n^{\mathrm{II}}=e^{ix(y-W_1)/l_{B_2}^2}\left[\sum_m t_{mn}e^{ik_m^{\mathrm{II}(+)}(y-W_1)}\Phi_m^{\mathrm{II}(+)}(x)\right] \tag{2b}$$

in region II, as well as

$$\Psi_n^{\mathrm{III}}=\sum_j [a_{jn}f_j(y)\sin k_j'(x-W_2)+c_{jn}g_j(x)\sin k_j''y] \tag{2c}$$

in the corner region. Here, $f_j(y)=\sqrt{2/W_1}\sin(j\pi y/W_1)$ represents the transverse wave function of electron in mode j at zero field in wire I, and $g_j(x)=\sqrt{2/W_2}\sin(jx\pi/W_2)$ is the transverse wave function of electron in mode j at zero field in wire II. The wave numbers $k_j'=[k_F^2-(j\pi/W_1)]^{1/2}$ and $k_j''=[k_F^2-(j\pi/W_2)]^{1/2}$ are either real for propagating modes or pure imaginary for evanescent modes. l_B denotes the magnetic length given by $l_B=\sqrt{\hbar c/eB}$. The transverse wave functions Φ in the presence of magnetic field satisfy the following one-dimensional Schrödinger equations of an electron with the Fermi energy $E_F=\hbar^2k_F^2/2m^*$ (m^* is an isotropic effective mass, which is taken to be the value $m^*=0.067m_0$ for the GaAs layer) and charge $-e$:

$$\left[\frac{d^2}{dy^2}+k_F^2-\left(k_n^{\mathrm{I}(\pm)}-\frac{eB_1y}{\hbar c}\right)^2\right]\Phi_n^{\mathrm{I}(\pm)}(y)=0 \tag{3a}$$

in region I, and

$$\left[\frac{d^2}{dx^2}+k_F^2-\left(k_n^{\mathrm{II}(\pm)}+\frac{eB_2x}{\hbar c}\right)^2\right]\Phi_n^{\mathrm{II}(\pm)}(x)=0 \tag{3b}$$

in region II. The magnetic field effect can be regarded as an additional effective potential introduced into the relevant Schrödinger equation. This effective magnetic potential can be expressed as

$$V_{\mathrm{eff}}(y)=\frac{\hbar^2}{2m^*}\left(k_n^{\mathrm{I}(\pm)}-\frac{eB_1y}{\hbar c}\right)^2 \tag{4a}$$

in region I, and

$$V_{\text{eff}}(x)=\frac{\hbar^2}{2m^*}\left(k_n^{\text{II}(\pm)}+\frac{eB_2x}{\hbar c}\right)^2 \tag{4b}$$

in region II.

To solve Eqs. (3a) and (3b), we expand the wave functions in terms of a set of complete bases, separately corresponding to the transverse eigenfunctions of the LQW in regions I and II at zero field as

$$\Phi_n^{\text{I}(\pm)}(y)=\sum_j \xi_{jn}^{\text{I}(\pm)} f_j(y), \tag{5a}$$

and

$$\Phi_n^{\text{II}(\pm)}(x)=\sum_j \eta_{jn}^{\text{II}(\pm)} g_j(x). \tag{5b}$$

With the use of an expanded basis,[35,36] for a given Fermi energy E_F, we obtain a set of eigenwave numbers $(k_n^{\text{I}(\pm)})$ [or $(k_n^{\text{II}(\pm)})$] and eigenwave functions $[\Phi_n^{\text{I}(\pm)}(y)]$ {or $[\Phi_n^{\text{II}(\pm)}(x)]$}. The group velocities of the jth state in regions I or II are, respectively,

$$v_j^{\text{I}(\pm)}=\frac{\hbar}{m^*}\int_0^{W_1}\Phi_j^{*\text{I}(\pm)}(y)\left(k_j^{\text{I}(\pm)}-\frac{eB_1y}{\hbar c}\right)\Phi_j^{\text{I}(\pm)}(y)dy, \tag{6a}$$

and

$$v_j^{\text{II}(\pm)}=\frac{\hbar}{m^*}\int_0^{W_2}\Phi_j^{*\text{II}(\pm)}(x)\left(k_j^{\text{II}(\pm)}+\frac{eB_2x}{\hbar c}\right)\Phi_j^{\text{II}(\pm)}(x)dx. \tag{6b}$$

Expansions [Eqs. (5a) and (5b)] involve an infinite sum including all possible evanescent modes. In practice, this sum must be truncated at some finite number, large enough to achieve a desired accuracy. We checked numerical convergence by flux conservation. The relationship $\Sigma_j(\tilde{t}_{jn}+\tilde{r}_{jn})=1$ should be persisted well, where $\tilde{t}_{jn}$ represents the transmission probability from incident mode n to final mode j and $\tilde{r}_{jn}$ is the reflection probability:

$$\tilde{t}_{jn}=\frac{v_j^{\text{II}(+)}}{v_n^{\text{I}(+)}}|t_{jn}|^2, \quad \tilde{r}_{jn}=\frac{|v_j^{\text{I}(-)}|}{v_n^{\text{I}(+)}}|r_{jn}|^2. \tag{7}$$

The transmission probability for individual given incident mode, for instance, for the incident electrons coming from the nth mode in region I, is given by

$$T_n=\sum_{j=1}^{N_2}\tilde{t}_{jn}, \tag{8}$$

where N_2 is the number of propagating modes in region II. The total transmission probability T is calculated by

$$T(E_F)=\sum_{n=1}^{N_1}T_n, \tag{9}$$

where N_1 is the number of propagating modes in region I. In the linear-response regime, the bent magnetoconductance of the LQW can be evaluated from the two-terminal Landauer–Büttiker formula,[37]

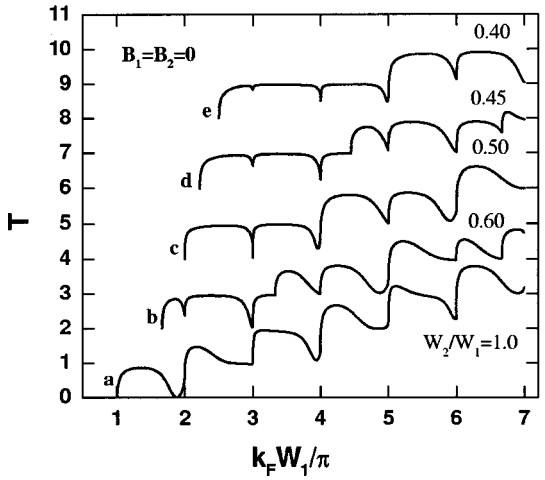

FIG. 2. Variation of total transmission probability T as a function of the Fermi wave number k_F of the incident electrons at zero field for different ratios of W_2-to-W_1 of the bent quantum waveguide. Hereafter, we always choose $W_1=2000$ Å in calculations. Curves $a-e$ correspond to $W_2/W_1=1.0$, 0.6, 0.5, 0.45, and 0.4, respectively. Two consecutive curves are separated for clarity.

$$G(E_F)=\frac{2e^2}{h}T(E_F). \tag{10}$$

III. RESULTS AND ANALYSES

A. Transmission of electrons in an L-shaped quantum waveguide at zero magnetic field

We first describe the variation of the total transmission probability T or conductance G as a function of the Fermi wave number k_F of the incident electrons at zero field for different ratios of W_2-to-W_1 of the LQW. The calculated transmission spectra are depicted in Fig. 2. Hereafter, we choose $W_1=2000$ Å in calculations. However, all the results possess scaling invariance: When $W\rightarrow\alpha W$ and at same time $B\rightarrow B/\alpha^2$, the normalized effective magnetic potential remains unchanged [see, Eqs. (4a) and (4b)]. Curves $a-e$ correspond to $W_2/W_1=1.0$, 0.6, 0.5, 0.45, and 0.4, respectively. Two consecutive curves are vertically separated by 2.0 for clarity. For an image-reflection symmetric structure under reflection about the diagonal intersection line of the corner, i.e., $W_1=W_2$, the quantized conductance step as shown in the curve a of Fig. 2 still seems to be observable as a new channel opens. We can always find a valley located just before the opening of a new channel. The wider valleys are shallower, this is in contrast to the narrower valleys which are deeper. They occur alternately on the curve. We can always find a valley located just before the opening of a new channel. The wider valleys are shallower, this is in contrast to the narrower valleys which are deeper. They occur alternately on the curve. For this structure, owing to the presence of the 90° bend at the corner of the LQW, the strong scattering of electrons with these energies by the corner leads to a substantial enhancement of the reflection.[4,13–19] Roughly speaking, this bend quantum waveguide is analogous to a narrow–wide–narrow structure.[38,39] The bend of the LQW is equivalent to introducing an effective longitudinal modula-

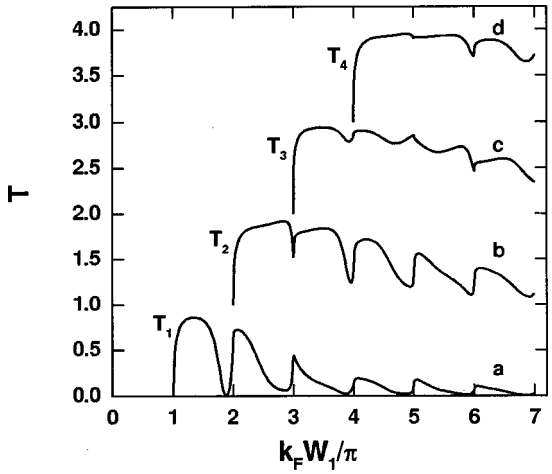

FIG. 3. Transmission spectra for four lowest modes of incident electrons in the image-reflection symmetric structure. Curves $a-d$ correspond to T_1-T_4, respectively.

tion potential. Two effective barriers are formed at the exits of cavity. The coupling between the incident mode and the mode in the cavity leads to the appearance of the valleys or dips in the transmission spectrum. The stronger the coupling is the broader the width of the valley. The origin of these valleys in transmission might be attributed to the mode–mode coupling as we will see in Fig. 3.

We now study the effect of the narrowing of width W_2 of wire II on the transmission spectrum. The effects are included by the following fourfolds: (1) The threshold wave number of the onset of conductance shifts toward the high wave number region, because it is determined by the smaller values between W_1 and W_2, and thus at present, inversely proportional to W_2. (2) The positions of all the valleys remain unchanged. However, these valleys are narrowed because the mode–mode coupling becomes weak as decreasing W_2. One can also note that the valley for the lower incident electron energy, e.g., the left most valley, gradually disappears as W_2 is decreased. This is reasonable that the disappearance of the left most valley owes to the increase of the onset of the conductance as W_2 is decreased. (3) When W_2 is shrunk, the width of the conductance plateaus of each curve gradually becomes wider by combining the adjacent ones together. However, the positions of reflection dips are still unchanged. Consequently, the width of the new plateau is equal to W_1/W_2, and each new plateau contains more dips. (4) As W_2 is decreased, an unusual variation of the plateau might occur, e.g., in curves *b* and *d* of Fig. 2, some plateaus develop into bumps while their next neighbor plateau reduces its height. This process continues until the combination of two plateaus is complete.

To reveal the origin of these valleys in transmission, we prefer to show the individual contribution of the lowest four modes to the transmission. Figure 3 displays the transmission probability of individual incident mode for the image-reflection symmetric structure. Curves *a, b, c,* and *d* correspond to T_1 for mode 1, T_2 for mode 2, T_3 for mode 3, and T_4 for mode 4, respectively. Two consecutive curves are offset by an amount of 1.0 for clarity. Compared with curve *a* in Fig. 2 and curves *a, b, c,* and *d* in Fig. 3, it is evident that transmission valleys are essentially originated from mode 1 and mode 2 in the wires. These valleys are nearly located at the wave numbers $k_F W_1/\pi =$ integer. For those modes with larger indices, the corresponding energy levels are higher than the height of the effective potential barriers at the exits of the cavity, therefore, the coupling effect becomes weak; no strong reflection peak takes place. Their corresponding transmission exhibits oscillation structures with small amplitude superimposed upon a declined straight line with small slope. Therefore, one may conclude that the mode–mode coupling might be the possible mechanism for the origin of the valleys. These results support the previous conclusions that the valleys are naturally originated from the mode–mode coupling effect.[40–42]

We now discuss the opposite case, i.e., W_2 is larger than W_1. The pattern of the transmission spectrum is similar with the case of narrowing wire II. If two structures have inverse ratios of W_2/W_1, for instance, one structure has $W_2/W_1 = 0.5$, and the other structure has $W_2/W_1 = 2.0$, by using different abscissa scales, for instance, one is measured by $k_F W_1/\pi$ for the former, and the other is $k_F W_2/\pi$ for the latter. It is found that two curves completely coincide with each other.

B. Transmission of LQW under inhomogeneous magnetic fields

We now investigate the influence of the perpendicular magnetic fields applied to the wire parts on the transmission properties of the LQW. The magnetic field on the corner region of the LQW is kept at zero. This means that a magnetically defined cavity is formed on the corner. In this article, we only concern ourselves with this special structure. Figure 4(a) shows the variation of single-mode transmission probability T_1 for the incident electrons coming from region I in the first subband as a function of the Fermi wave number. The parameters are: $W_1 = W_2$ and $B_1 = B_2$. Curves $a-e$ correspond to different magnetic field strengths as $B = 0$, 0.2, 0.4, 0.6, and 0.8 T (Tesla), respectively. Two consecutive curves are offset by an amount of 1.0 for clarity. At zero field (curve *a*), the transmission increases from zero to its first broad bump with a maximum 0.86, and subsequently, drops into a zero-transmission valley, originating from the strong scattering of electrons on the corner. As applying the magnetic fields to the two wires, the transmission spectrum is substantially modified. Sharp transmission peaks with unity amplitude and deep dips emerge as shown in curves $b-e$. The action of the magnetic fields is equivalent to the formation of two magnetic barriers at the exits of the cavity. The electrons inside the cavity are subjected to multiple reflections from the abrupt magnetic-field changes at interfaces.[27,28] It leads to the creation of peak-dips structures in transmission. When increasing the magnetic field, the first subband level in the wires is lifted. This results in the threshold wave number of the transmission being shifted to the right. When the position of the first valley remains fixed, therefore, the bump is gradually narrowed and develops a peak until the first valley is finally merged or disappears at a certain high field as shown in curve *d*. At the field strength

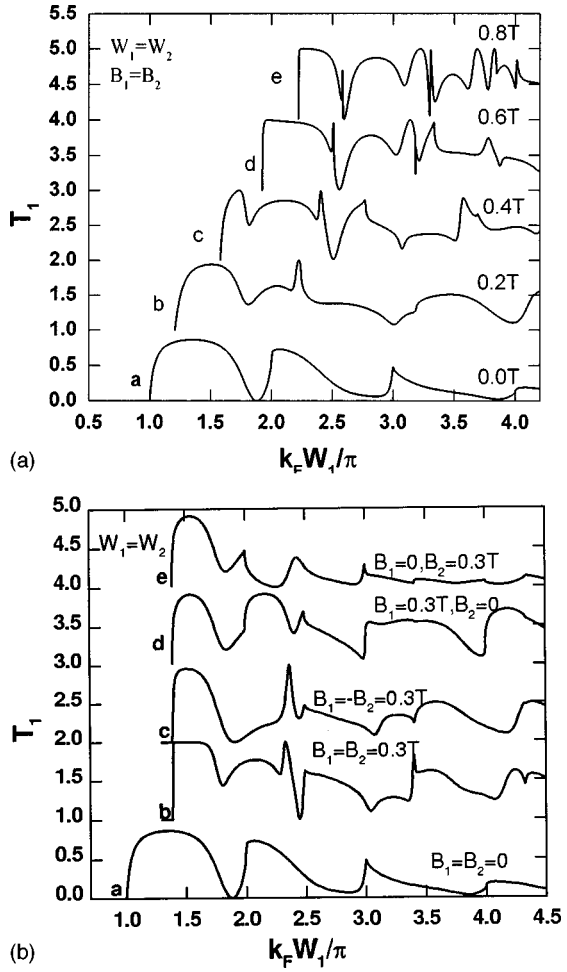

FIG. 4. Dependence of the single-mode transmission probability T_1 on the Fermi wave number, (a) for different magnetic field strengths when $B_1=B_2=B$, and (b) for different magnetic configurations. We assume $W_1=W_2$. Curves $a-e$ in (a) correspond to $B=0$, 0.2, 0.4, 0.6, and 0.8 T. Curves $a-e$ correspond to different magnetic confinement configurations: at zero field for curve *a*, $B_1=B_2=0.3$ T for curve *b*, $B_1=-B_2=0.3$ T for curve *c*, $B_1=0.3$ T and $B_2=0$ for curve *d*, and $B_1=0$ and $B_2=0.3$ T for curve *e*. Two consecutive curves are offset for clarity.

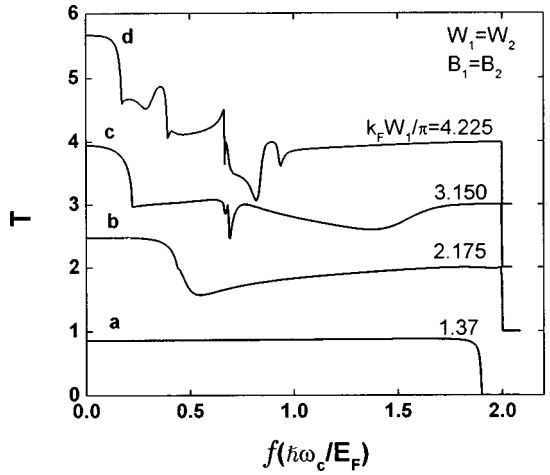

FIG. 5. Variation of total transmission probability T with magnetic fields only subject to the wires in the LQW with symmetric structure for different incident electron energies. $W_1=W_2=2000$ Å and $B_1=B_2=B$. Curves $a-d$ correspond to $k_FW_1/\pi=1.37$, 2.175, 3.150, and 4.225, respectively. The curves are offset for clarity.

0.2 T, one transmission peak with unity amplitude is observed. As the field strength B increases, the peak-dip pair or dip-peak pair structures appear. At higher field, 0.8 T, many sharp peaks and dips occur. These resonant structures are primarily ascribed to the mode-mode coupling effect and the multiple reflection of electrons waves inside the cavity.[27,28] It follows that the transmission properties of electrons in the LQW can be remarkably improved by adjusting magnetic fields in wires.

We now investigate the effect of different magnetic configurations on the single-mode transmission T_1 in detail. We still focus on the LQW with symmetric structure. The calculated transmission spectra of T_1 are shown in Fig. 4(b). Two consecutive curves are offset by an amount of 1.0 for clarity. Curves $a-e$ correspond to different magnetic configurations: curve *a* for zero-field case, curve *b* for $B_1=B_2=0.3$ T, curve *c* for $B_1=0.3$ T, and $B_2=-0.3$ T, curve *d* for $B_1=0.3$ T and $B_2=0$, and *e* for $B_2=0.3$ T and $B_1=0$. It is clearly seen that the threshold wave number keeps unchanged for all curves $b-e$. For finite field with the same polarity in the wires, the cavity is magnetically well defined, thus, sharp peaks and dips are observed. However, when reversing the polarity of the field in one wire with respect to the other wire, the peak-dip structures in T_1 disappear and are remarkably smeared, in particular, in high energy region (curve *c*). For the output wire with zero field, oscillations in T_1 are obviously enhanced (curve *d*). When exchanging the magnetic distributions in the two wires, i.e., assuming $B_1=0$ and $B_2=0.3$ T, in contrast to curve *d*, the oscillations are remarkably suppressed (curve *e*), and the transmission decays to zero at high energy region. It is seen from Eqs. (4a) and (4b) that the effective magnetic potential of electrons depends on the $k_n^{\mathrm{I,II}(\pm)}$, the magnitude and polarity of $B_1(B_2)$. Consequently, it is expected that any change of the magnetic configurations should substantially modify transmission behaviors of the LQW.

To further examine the influence of the magnetic field on the transmission spectrum, we study the effect of the depletion process of the high-lying modes on total transmission probability T as increasing field. Figure 5 shows the T as a function of $f=\hbar\omega_c/E_F$ for four different incident electron energies in the LQW with $W_1=W_2$ and $B_1=B_2=B$. Where $\omega_c=eB/m^*c$ is the cyclotron angular frequency of electrons in magnetic field. Curves $a-d$ correspond to $k_FW_1/\pi=1.37$, 2.175, 3.150, and 4.225, respectively. The numbers of the propagating modes in wires at zero field are 1, 2, 3, and 4, respectively. Two consecutive curves are vertically offset by an amount of 1.0 for clarity. Since the Landau quantization level is dominant over the threshold energy of the onset of transmission, the jth mode is completely depleted when $f=1/(j-0.5)$, and so the overall transmission ceases when $f>2$.[25,26] When only the lowest mode is occupied (curve *a*), during the magnetic depletion process of this mode no structure appears in transmission T. When two propagating modes exist in the wires, as increasing the magnetic field, the high-lying mode is first depleted, hence the transmission abruptly drops to a valley at $f=0.494$. Passing over this valley, the transmission increases monotonically

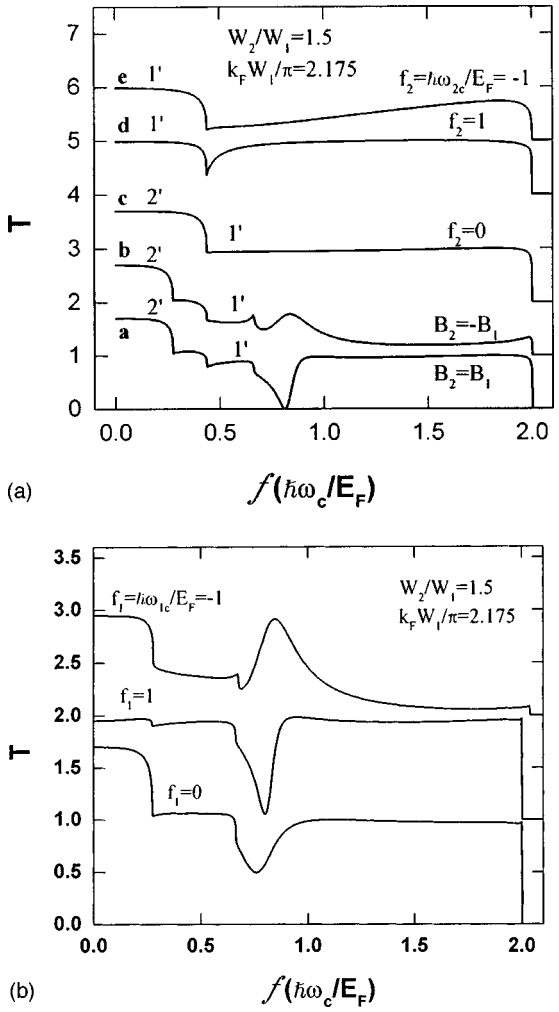

FIG. 6. Variation of total transmission probability with the magnetic field in the LQW with asymmetric structure for different magnetic configurations. $W_2/W_1=1.5$. Curves $a-e$ in (a) correspond to $B_2=B_1$ for curve *a*, $B_2=-B_1$ for curve *b*, $f_2=\hbar\omega_c(B_2)/E_F=0$, 1, and -1 for curve $c-e$, respectively. Curves $a-c$ in (b) correspond to $f_1=\hbar\omega_c(B_1)/E_F=0$, 1, and -1, respectively. The incident electron wave number is fixed at $k_FW_1/\pi=2.175$. The curves are offset for clarity.

and approaches unity, and dramatically ceases at $f=2$, all the modes are depleted. As the number of occupied modes is increased, the transmission behaviors exhibit complicated oscillation structures containing many peaks–valleys. The interference of the wave functions associated with different channels are responsible for these oscillation structures (curve *d*).

We now further describe the transmission features of the LQW with asymmetric structure during the magnetic depletion process of the modes. We consider an LQW with $W_2/W_1=1.5$. The variation of total transmission probabilities for different magnetic configurations with a fixed wave number $k_FW_1/\pi=2.175$ is plotted in Figs. 6(a) and 6(b). Curves in Fig. 6(a) are functions of B_1 which is converted to the parameter $f=\hbar\omega_c/E_F$, and correspond to different magnetic fields of B_2: curve *a* to $B_2=B_1=B$, curve *b* to $B_1=-B_2=B$, curve *c* to $B_1=B$ with $B_2=0$, curve *d* to $B_1=B$ with $f_2=\hbar\omega_{c2}/E_F=1$, and curve *e* to $B_1=B$ with $f_2=-1$. Where $\omega_{c2}=eB_2/m^*c$ is the cyclotron frequency of electrons in magnetic field and f_2 can be viewed as a normalized strength of magnetic field applied to the wire region II. Under these conditions we mentioned above, there are two (one) active propagating modes (mode) in the wires for the cases $a-c(d-e)$ when applied field is zero or weak. As $f=\hbar\omega_c/E_F$ increases, step variation of the transmission probabilities occurs until all the propagating modes are depleted. For clarity, *b* and *c* are offset by 1 and 2, while in the cases *d* and *e* the curves are shifted by 4 and 5. For the case $B_2=B$ (curve *a*), the transmission drops from $T=2'$ step to $T=1'$ step as increasing *B*, electrons are then experienced from strong reflection, thus one valley appears near $f=0.8$. Subsequently, transmission monotonically increases up to $T=1'$ step again and finally drops to zero at $f=2$. When reversing the polarity of B_2 with respect to B_1, the transmission valley becomes quite shallow and $T=1'$ step in the high field region disappears (curve *b*). When fixing $B_2=0$ and scanning B_1, i.e., the magnetically confined cavity is now completely opened at the upper exit, no valley is observed in transmission (curve *c*). When applying a finite field to wire II, i.e., $f_2=1$, a quite narrow dip brings out at a low field (curve *d*). However, when inverting the sign of B_2, this valley becomes obscure (curve *e*).

We now consider opposite cases, that is $B_2=B$ with fixed $k_FW_1/\pi=2.175$. Curves *a*, *b*, and *c* in Fig. 6(b) show the dependence of *T* on the magnetic field *f* which denotes the strength of B_2, for different values of B_1: $B_1=0$, $f_1=\hbar\omega_{c1}/E_F=1$, and -1, respectively. Similarly, we denote $\omega_{1c}=eB_1/m^*c$. The application of the magnetic field B_1 lifts the subband levels of electrons in wire I. As increasing *f*, the height of the effective magnetic barrier at the upper exit of the cavity is increased; thus, the strong reflection appears at some magnetic field, it results in the appearance of a dip. For larger *f*, this dip becomes deep and narrow. However, when reverting the sign of B_1, this dip is converted into a transmission peak, comparing curves *b* and *c*. From these results, it concludes that by changing the magnetic configurations in the LQW, its transmission characteristics can be flexibly controlled. Therefore, it is expected that one can tailor transmission spectrum of the LQW to match the practical requirements by designing appropriate magnetic configuration.

IV. SUMMARY

We have studied transmission properties in an L-shaped quantum waveguide LQW subject to an inhomogeneous magnetic field perpendicular to the LQW plane. The magnetic field is kept zero at the corner region, thus, a magnetically defined cavity is formed in the LQW. We calculate the total transmission probability of electrons for different ratios of W_2-to-W_1 in the LQW at zero field. The profile of the transmission spectrum as a function of the incident electron energy is gradually developed. The wide valleys become sharp dips and the conductance plateaus are expanded. However, the positions of all the valleys remain unchanged. It implies that these valleys are essentially ascribed to the 90° bend in the LQW in the corner of LQW electrons are experienced from strong scattering and reflection and leads to the

appearance of the valleys. The bent quantum waveguide is analogous to a narrow–wide–narrow structure. The coupling between the mode in wires and the mode in cavity becomes weak as narrowing the output wire. As a consequence, the width of valleys is decreased. From the analyses of the transmission of individual incident modes, we confirm that the valleys originated from the contributions of the two lowest modes.

We investigated the influence of the magnetic fields only subject to the wires on transmission properties of the LQW. A magnetically defined cavity is formed on the corner region. We find that transmission characteristics of electrons in the LQW strongly depend on magnetic configurations. Sharp peaks with unity amplitude and deep dips emerge in single-mode transmission spectrum at finite fields. The mode–mode coupling between the wires and the cavity and multiple reflection of electrons in the cavity are responsible for these structures. Single-mode transmission spectrum depends sensitively on magnetic configurations. We study the development of total transmission probability with magnetic field for different incident electron energies and various magnetic configurations. In magnetic depletion process of the propagating modes, one can observe various patterns in transmission, such as stepped drop, wide valley, deep dips, large oscillations, or without any structure. From these results, it is believed that by applying an inhomogeneous magnetic field to the LQW and designing an appropriate magnetic configuration may provide another available way to control transmission property of the LQW to match practical requirements in devices.

ACKNOWLEDGMENTS

One of the authors (B. Y. Gu) is grateful for the hospitality of the National Science Council, Taiwan and the Electrophysics Department, National Chiao Tung University, Hsinchu, Taiwan. This work was supported by National Science Council, Taiwan, under Grant No. NSC 88-2112-M-009-004.

[1] C. W. J. Beenakker and H. van Houton, in *Solid State Physics: Semiconductor Heterostructures and Nanostructures*, edited by H. Ehrenreich and D. Turnbull (Academic, New York, 1991), Vol. 44, p. 1, and references cited therein.
[2] B. Ricco and M. Y. Azbel, Phys. Rev. B **29**, 1970 (1983).
[3] M. W. Dellow, P. H. Beton, C. J. G. Langerak, T. J. Foster, P. C. Main, L. Eaves, M. Henini, S. P. Beaumont, and C. D. W. Wilkinson, Phys. Rev. Lett. **68**, 1754 (1992).
[4] F. Sols, M. Macucci, U. Ravaioli, and K. Hess, Appl. Phys. Lett. **54**, 350 (1989); J. Appl. Phys. **66**, 3892 (1989); F. Sols and M. Macucci, Phys. Rev. B **41**, 11887 (1990).
[5] J. A. del Alamo and C. C. Eugster, Appl. Phys. Lett. **56**, 78 (1990).
[6] C. C. Eugster, J. A. del Alamo, M. J. Rooks, and M. R. Melloch, Appl. Phys. Lett. **60**, 642 (1992); Phys. Rev. B **46**, 10146 (1992); **48**, 15057 (1993); Phys. Rev. Lett. **67**, 3586 (1991).
[7] R. Q. Yang and J. M. Xu, Phys. Rev. B **43**, 1699 (1991).
[8] J. Q. Wang, S. Q. Yuan, B. Y. Gu, and G. Z. Yang, Phys. Rev. B **44**, 13618 (1991).
[9] J. Q. Wang, B. Y. Gu, and G. Z. Yang, J. Appl. Phys. **72**, 2299 (1992); Phys. Rev. B **47**, 13442 (1993).
[10] Y. Takagaki and K. Ploog, Phys. Rev. B **49**, 1782 (1994).
[11] J. Wang, H. Guo, and R. Harris, Appl. Phys. Lett. **59**, 3075 (1991).
[12] J. Wang, Y. J. Wang, and H. Guo, Phys. Rev. B **46**, 2420 (1992); **47**, 4348 (1993).
[13] C. S. Lent, Appl. Phys. Lett. **56**, 2554 (1990).
[14] R. L. Schult, D. G. Ravenhall, and H. W. Wyld, Phys. Rev. B **39**, 5476 (1989).
[15] J. Goldstone and R. L. Jaffe, Phys. Rev. B **45**, 14100 (1992).
[16] P. Exner and P. Seba, J. Math. Phys. **30**, 2574 (1989).
[17] J. Wang and H. Guo, Appl. Phys. Lett. **60**, 654 (1992).
[18] J. P. Carini, J. T. Londergan, K. Mullen, and D. P. Murdock, Phys. Rev. B **46**, 15538 (1992).
[19] J. P. Carini, J. T. Londergan, K. Mullen, and D. P. Murdock, Phys. Rev. B **48**, 4503 (1993).
[20] J. E. Müller, Phys. Rev. Lett. **68**, 385 (1992).
[21] D. B. Chklovskii, Phys. Rev. B **51**, 9895 (1995).
[22] B. Y. Gu, W. D. Sheng, X. H. Wang, and J. Wang, Phys. Rev. B **56**, 13434 (1997).
[23] H. S. Sim, K. H. Ahn, K. J. Chang, G. Ihm, N. Kim, and S. J. Lee, Phys. Rev. Lett. **80**, 1501 (1998).
[24] I. S. Ibrahim, V. A. Schweigert, and F. M. Peeters, Phys. Rev. B **56**, 7508 (1997); Superlattices Microstruct. **22**, 203 (1997).
[25] B. L. Altshuler and L. B. Ioffe, Phys. Rev. Lett. **69**, 2979 (1992); T. Sugiyama and N. Nagoasa, *ibid.* **70**, 1980 (1993); S.-C. Zhang and D. P. Arovas, *ibid.* **72**, 1886 (1994).
[26] Z. L. Ji and D. W. L. Sprung, Phys. Rev. B **54**, 8044 (1996); **56**, 1045 (1997).
[27] H. Yoshioka and Y. Nagaoka, J. Phys. Soc. Jpn. **59**, 2884 (1990).
[28] Y. Takagaki and K. Ploog, Phys. Rev. B **51**, 7017 (1995); **53**, 3885 (1996).
[29] H. Xu, Phys. Rev. B **52**, 5803 (1995).
[30] X. Q. Li and F. M. Peeters, Superlattices Microstruct. **22**, 243 (1997); X. Q. Li, F. M. Peeters, and A. K. Geim, J. Phys.: Condens. Matter **9**, 8065 (1997).
[31] M. A. McCord and D. D. Awschalom, Appl. Phys. Lett. **57**, 2153 (1990).
[32] M. L. Leadbeater, S. J. Allen, Jr., F. DeRosa, J. P. Harbison, T. Sands, R. Ramesh, L. T. Florez, and V. G. Keramidas, J. Appl. Phys. **69**, 4689 (1991); K. M. Krishnan, Appl. Phys. Lett. **61**, 2365 (1992); R. Yagi and Y. Iye, J. Phys. Soc. Jpn. **62**, 1279 (1993).
[33] A. Matulis, F. M. Peeters, and P. Vasilopoulos, Phys. Rev. Lett. **72**, 1518 (1994).
[34] S. J. Bending, K. von Klitzing, and K. Ploog, Phys. Rev. Lett. **65**, 1060 (1990); A. K. Geim, Pis'ma Zh. Eksp. Teor. Fiz. **50**, 359 (1989) [JETP Lett. **50**, 389 (1990)].
[35] H. Tamura and T. Ando, Phys. Rev. B **44**, 1792 (1991).
[36] S. Chaudhuri and S. Bandyopadhyyay, J. Appl. Phys. **71**, 3027 (1992).
[37] M. Büttiker, Phys. Rev. B **38**, 9375 (1988).
[38] A. Szafer and A. D. Stone, Phys. Rev. Lett. **62**, 300 (1989).
[39] Y. Avishai and T. B. Band, Phys. Rev. B **41**, 3253 (1990).
[40] Y. Takagaki and D. K. Ferry, Phys. Rev. B **45**, 13494 (1992).
[41] S. A. Gurvitz and Y. B. Levinson, Phys. Rev. B **47**, 10578 (1993); Y. B. Levinson, M. I. Lubin, and E. V. Sukhorukov, *ibid.* **45**, 11936 (1992).
[42] P. J. Price, Phys. Rev. B **48**, 17301 (1993); Semicond. Sci. Technol. **9**, 899 (1994).